

## Two-dimensional numerical modelling of slamming impact loads on high-speed craft

Josef Camilleri<sup>1,\*</sup>, Pandeli Temarel<sup>1</sup> and Dominic Taunton<sup>1</sup>

<sup>1</sup> Fluid Structure Interactions Group, University of Southampton, UK

**Abstract.** The constant velocity impact of a flexible panel with water is simulated by using the computational fluid dynamics code Star CCM+ coupled with the finite element code ABAQUS. A detailed description of the numerical model is given, and issues with numerical stability are discussed. The influence of different structural boundary conditions in the two-dimensional model is examined. The effects of hydroelasticity on the fluid loading are discussed by comparing the results from hydroelastic and rigid body simulations. Comparisons with published experimental data show favourable agreement for the test case investigated.

**Keywords:** *slamming; high-speed craft; numerical modelling; co-simulation; CFD; FEA*

### 1. Introduction

High-speed craft such as patrol, military, and rescue craft often have to travel at their highest speed possible in relatively rough seas. In such conditions, the craft frequently launches off waves, emerging from the water, and then slams back onto the free surface with a high relative velocity. The slam induced loads acting on the hull structure upon re-entry constitute a significant portion of the design loads and are generally the primary reason for crew injuries and structural failures, either due to fatigue loading or catastrophic hull failures during an extreme event. Accurate prediction of these impact loads and structural responses is therefore crucial for safe, reliable and efficient structural design.

Traditionally, hull-water impacts have been investigated by analysing the simplified problem of a two-dimensional (2D) hull section impacting an initially calm water surface. Generally, the structure has been assumed rigid and the hydrodynamic loading and structural responses have been treated separately, neglecting the influence of the flexibility of the structure on the fluid loading. However, in many cases hydroelastic effects can have a significant influence and strongly coupled analyses are required. Various criteria for determining when hydroelastic effects need to be considered have been presented [1, 2, 3]. The basis of these criteria is that

---

\* Correspondence to: jc1d13@soton.ac.uk

hydroelastic effects can be neglected if the loading period is significantly larger than the natural period of vibration of the structure.

Several investigations on the hydroelastic impact problem, using a wide range of methods, have been published. Maki et al [4] studied the constant velocity impact of an elastic wedge using one way coupling of the open source computational fluid dynamics (CFD) solver OpenFOAM and the dynamic finite element (FE) method. Acoustic elements were used to represent the added mass due to flexure. The deflections show good agreement with published theoretical results in terms of peak value; however, there is a large time lag between maxima, due to the structure assumed wet. Piro & Maki [5] further improved their method by adopting a two-way coupling procedure. The predicted stress time histories are compared with the one-way coupled results and a rigid/quasi-static (RQS) solution. The strongly coupled method agrees well with the one-way coupled method; however, the RQS solution was found to predict lower stress levels for all plate thicknesses tested. Stenius et al [6] investigated the influence of hydroelastic effects on the structural response using the commercial FE code LS-DYNA. Hydroelastic solutions are compared with corresponding RQS solutions in order to quantify the influence of hydroelastic effects. The RQS solution was found to yield larger deflections during the initial phases of impact, whereas the hydroelastic solution gives larger deflections later in time. This phase lag is linked with both kinematic and inertia related hydroelastic effects. Thus, depending on the impact period considered (chines-dry or chines-wet conditions), hydroelastic effects can contribute to reduce or increase the structural responses. Other numerical techniques used to study the hydroelastic problem include coupled boundary element methods (BEM) and FE methods (e.g. [7]), coupled smoothed particle hydrodynamics (SPH) and FE methods (e.g [8]) and Arbitrary Lagrangian-Eulerian (ALE) methods (e.g. [9]).

Experiments with flexible structures have also been performed. Battley et al [10] studied the effect of panel stiffness on the response of composite hull panels. Significant kinematic hydroelastic effects such as change in local deadrise angle at the chine, and panel velocity at the centre, and associated increase in fluid loading were observed, particularly for the most flexible panel. Despite this increase fluid loading, the scaled panel responses are smaller for the more flexible panel suggesting that hydroelastic inertia effects also have an effect. A similar, but more comprehensive experimental study was carried out by Allen [11], see section 3.1. Luo et al [12] dropped an idealized segment of a ship structure including the internal framing. Peak strain responses were found to increase with increasing panel flexibility, followed by high frequency vibrations. Panciroli et al [8] studied the influence of panel thickness, deadrise angle and impact velocity on the impact-induced strains on composite and aluminium wedges. The importance of hydroelastic effects was found to be governed by the ratio between the loading and natural periods of the structure.

In this paper, the constant velocity impact of a flexible panel with water is studied using a fully coupled 2D CFD-FE method. A detailed description of the numerical model is given and issues with numerical stability are discussed. The influence of the structural boundary conditions on the fluid loading and structural response is studied. The predicted pressures and deflections are compared against the experimental data of Allen [11], showing relatively good agreement. The pressures predicted by the coupled CFD-FE method are also compared with a rigid body impact model.

## 2. Numerical solution method

The computations presented in this paper are performed using the CFD solver Star CCM+ coupled with the FE solver Abaqus in a two-way manner. A brief summary of the numerical solution method is given here. More details can be found in the Star CCM+ user guide [13].

Star CCM+ uses the Finite Volume method to transform the governing equations i.e., the Navier-Stokes (N-S) equations, into a system of algebraic equations that can be solved numerically. The solution domain is first divided into a finite number of control volumes, of any polyhedral shape, with local refinements in the region of interest. The time period is also divided into a finite number of time steps. The governing equations are approximated for each control volume using 2<sup>nd</sup> order accurate approximations. An implicit time-stepping scheme is used as it allows for larger time steps and provides better stability compared to explicit schemes. The time derivative is approximated using the first-order Euler scheme. The system of coupled non-linear equations is solved in a segregated iterative manner, following the SIMPLE algorithm.

The free surface is modeled using an interface capturing scheme of the Volume-of-Fluid (VOF) type, where its location is determined by solving an additional transport equation. The High-Resolution-Interface-Capturing (HRIC) is used to discretize the convective part of the volume fraction equation to achieve a sharp interface and avoid unphysical solutions.

In the present approach, the panel and grid are kept fixed in space, and the free surface moves with a constant velocity upwards towards the plate. This avoids unnecessary mesh deformation related to rigid body motion, and makes mapping of the data between the fluid and structure easier. Thus, the space conservation law, describing the conservation of volume when the mesh changes its shape or position must also be satisfied. The morphing motion model is used to deform the fluid grid to accommodate the structural deformations. It uses a multi-quadratic morphing model based on radial basis functions to define the motion of interior vertices, which originates from the motion of the vertices along the fluid-structure interface, that is, the panel surface.

Coupling between Star CCM+ and Abaqus is done using an implicit scheme as it allows multiple exchanges per coupling time step. For strongly coupled problems, implicit schemes are more stable, however at the expense of larger computational cost. At the fluid-solid interface Star CCM+ passes traction loads (pressure and wall shear stress) to Abaqus, and Abaqus passes nodal displacements to Star CCM+.

## 3. Elastic plate impact

### 3.1. Experiments of Tom Allen

Allen [11] conducted a detailed experimental investigation into the constant velocity impact of flexible composite hull panels with water. Experiments were performed using the Servo-hydraulic Slam Testing System (SSTS), which uses a

water tank measuring 3.5m in diameter, filled with water to 1.4m deep. A high-speed servo-hydraulic system is used to drive the test fixture and panel into the water, with a constant or time varying velocity. The panel deadrise angle can be changed from  $0^\circ$  to  $40^\circ$  in  $10^\circ$  increments. Fixed vertical panels at the sides and back of the test fixture are used to constrain the flow along the panel, creating symmetrical, 2D impact conditions.

Eight test specimens, covering a wide range of panel rigidity were tested. In this study only one test specimen is considered, a flexible foam-cored sandwich panel (Gurit® M100) with GRP skins, panel GM100. The panel has external dimensions of 1.03 m by 0.6 m with an unsupported region between the simply supported edges of the test fixture measuring 0.99 m by 0.485 m. Fabric straps and steel fittings are used to hold the panel against the test fixture frame and prevent in-plane motion, as shown in Figure 1(a) [11]. Panel properties and test conditions are outlined in Table 1.

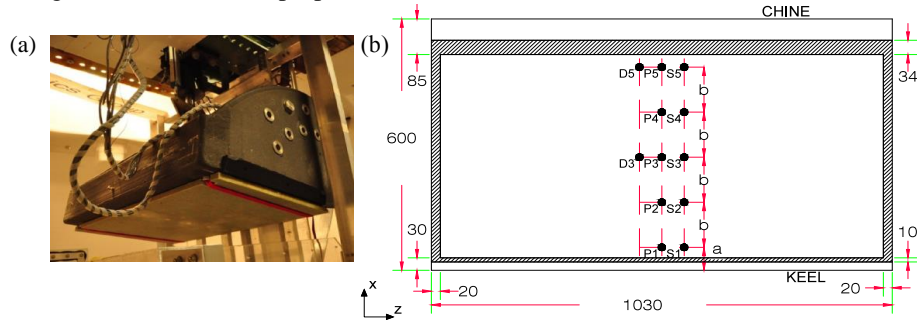


**Figure 1.** (a) Experimental set-up. (b) Schematic of the GM100 panel. Locations: P1 – P5 pressure sensors, S1 – S5 strain gauges and D3 and D5 displacement transducers. Shaded region is the panel-supporting frame. All dimensions are in mm.  $a = 55\text{mm}$  and  $b = 107.5\text{mm}$ .

**Table 1.** GM100 panel properties and test conditions.

Thickness (mm)	$t_f = 1.63, t_c = 14.0$
Weight (kg)	4.5
Bending stiffness D (kNm)	2.54
Shear stiffness S (kN/m)	722
Impact velocity (m/s)	1.0 – 6.0 (0.5 m/s increments)
Deadrise angle ( $^\circ$ )	10, 20, 30

The instrumentation includes dynamic pressure sensors, resistance strain gauges, displacement transducers, and a load cell. Pressures and strains are measured at five locations along panel, whereas deflection is measured at the center and chine as shown in Figure 1(b). Data is sampled at a rate of 51.2 kHz. Each test was repeated a minimum of three times. More details are given in Allen [11].

In the present work, only one test configuration is considered, a  $10^\circ$  deadrise angle panel impacting the water with a constant velocity of 1m/s.

### 3.2. Fluid model in Star CCM+

The geometry of the panel and tank are shown in Figure 2. The size of the numerical tank was extended to limit the influence of the boundaries on the solution. The half-width of the tank is 4.0 m (x-direction) and the height is 4.5 m (y – direction). The quasi-2D model has an in-plane thickness (z-direction) of 5 mm with a symmetry boundary condition on the front and back faces to ensure 2D flow. The boundary on the left is a symmetry plane, representing the fixed vertical plate in the experiments. A no-slip wall condition is applied on the test panel surface and the tank wall on the right side. The lower boundary is defined as velocity inlet, with the inflow velocity set equal to the panel velocity. The top boundary is set to pressure outlet, with atmospheric pressure conditions.

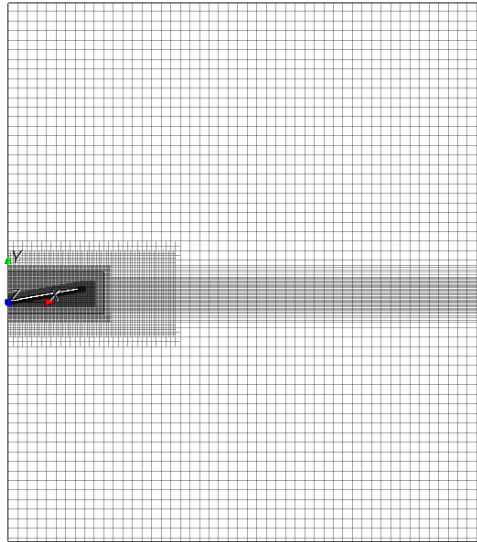


**Figure 2.** Geometry of the tank and panel and the trimmed hexahedral mesh in Star CCM+.

The solution domain is divided into two regions, a small rectangular region surrounding the panel, called the morphing region, where the fluid mesh moves to accommodate structural deformations, and a stationary region where the rest of the mesh remains fixed, as shown in Figure 3. This is done to reduce computational costs and improve the performance and stability of the solution.

The mesh is trimmed Cartesian with local refinements near the panel bottom and on the free surface, to accurately capture the highly localized peak pressure distribution and the large free surface deformations. The dimensions of the cells in the tangential and normal directions of the panel bottom are 2.5mm and 0.93mm respectively. The mesh becomes coarser towards the tank walls. Prism layers (high-aspect ratio cells) are added on the panel surface to accurately resolve the near wall flow features, such as jet formation and flow separation, as shown in Figure 3. The mesh has approximately 20,000 cells. No mesh sensitivity studies were performed. The chosen mesh sizes are based on the results of Camilleri et al [14].

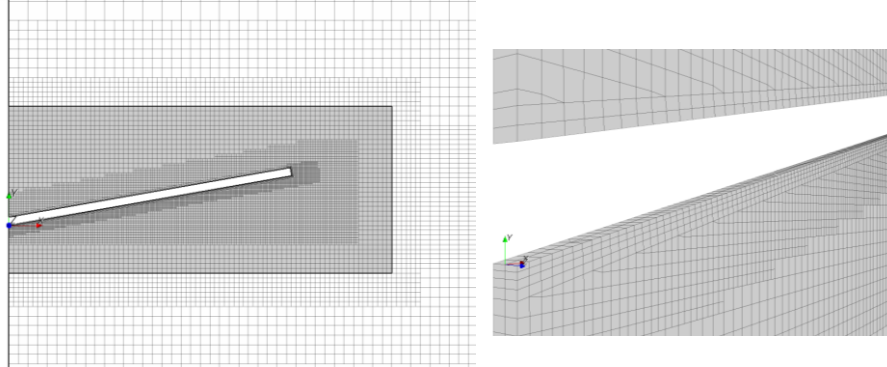


**Figure 3.** Partial views of the mesh showing the morphing (dark shaded) and stationary (light shaded) regions, local refinements and prism layers.

The flow is assumed to be viscous and laminar, meaning that the Navier-Stokes (N-S) equations are solved rather than the Reynolds averaged (RANS) equations. The duration of a typical slamming impact is too short for turbulence effects to develop [5]. Both water and air are treated as compressible fluids. The VOF multiphase model is used to account for the free surface and its arbitrary deformations. The initial position of the free surface is set to 0.05 m below the panel to allow for the flow to develop before impact. All computations were carried out with a constant time step of 0.04ms. The time step was chosen such that the Courant number is approximately 0.5 in the regions of interest. Furthermore, simulations with half the original time step showed negligible difference, indicating that the localized (in time) pressures are well resolved. The coupling time step size is also set to 0.04ms.

### 3.3. Structural model in ABAQUS

The structural model is 2D beam representation of the center span of the panel, see Figure 4. Modelling the panel as a beam should give reasonably accurate results provided that the aspect ratio of the panel is sufficiently high, as is the case [15]. The single-element-thick beam has a length of 600 mm and total thickness of 17.3 mm (skins and core) with the material properties given in Table 1.

The core and skins are meshed using 8-node linear solid elements (C3D8R). The element size along the panel is set to 2.5 mm to match as closely as possible the fluid and structure grids at the interface. The model has 3 elements through the thickness of each of the skins and five elements through the core as shown in Figure 5. In total, 2640 elements were used to mesh the panel.

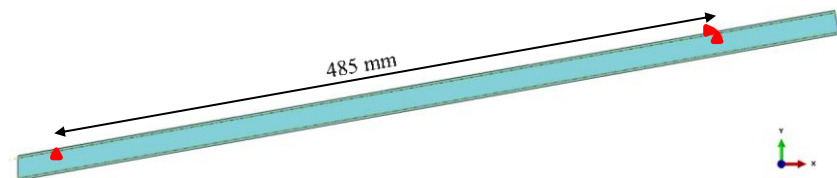


**Figure 4.** Beam model and point supports (red) in ABAQUS.

One of the main issues with modelling the panel as a 2D beam is how to accurately represent the experimental boundary conditions. In the experiments, the panel is held against the test fixture frame using straps at the ends. The conditions along the centerline of the panel are therefore not explicitly defined. To investigate the influence of the boundary conditions on the fluid loading and structural response two different models have been considered:

1. The beam is simply supported from two points 485 mm apart, representing the inner edges of the fixture frame in the SSTS with in-plane fixation at the chine edge to prevent rigid body motion, see Figure 4 and Figure 5(a).
2. The panel areas in contact with the fixture frame (shaded area in Figure 1(b)) are assumed to remain so during impact. These regions are set to have zero vertical displacement, with in-plane fixation at the chine edge, see Figure 5(b).

In both cases, a z-symmetry condition is applied on front and back faces of the beam. Gravity and geometrical nonlinear effects are also included in the model. Numerical damping with Moderate Dissipation settings is used [16]. The 1<sup>st</sup> dry natural frequency of the panel is 110.8 Hz and 145.3 Hz for the point and area supports respectively, which is close to the estimated value of 152 Hz [11, 15].

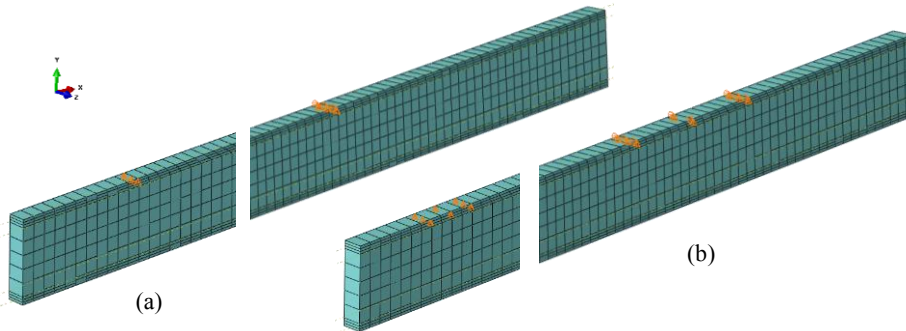


**Figure 5.** Close-up images of the structural model in ABAQUS showing the mesh and the (a) point and (b) area supports at the keel and chine ends.

## 4. Results and discussion

### 4.1. Numerical stability

Fluid-structure interaction problems are known to experience issues with numerical stability, particularly in problems where the added mass of the structure is comparable with the structural mass and/or the hydrodynamic loads and structural velocities change dramatically [17]. Two parameters that were found to have a significant influence on the solution stability are the number of iterations per time step and fluid compressibility.

The convergence of a solution depends on a number of factors including the time step size, order of scheme in space and time and also the number of iterations per time step. In strongly coupled problems more iterations are generally needed to achieve

convergence of the fluid forces at the interface, and maintain stability in the solution. The influence of the number of iterations per time step on the solution was studied in a systematic manner. The number of exchanges between the two solvers was also changed to study its effects on the solution. Table 2 summarizes the values tested. All simulations were carried using a 3.4 GHz core i7 single-processor PC.

**Table 2.** Iterations and exchanges per time step study.

Iterations/ time step	Exchanges/ time step	Iterations/ exchange	CPU time (hrs.)
12	3	4	4.16
20	4	5	6.44
40	5	8	14.96

Convergence of the pressure field is judged by monitoring the pressure over iterations within a time step at several discrete locations in the domain. The pressure and deflection time histories showed negligible difference, further suggesting that the temporal discretization errors are small and the chosen time step is correct. The stability of the pressure field was found to improve with increasing the number of iterations and exchanges. It was concluded that 20 iterations and 4 exchanges per time step are needed to achieve convergence for these particular test conditions.

The stability of the solution can be improved further by treating the flow as compressible. In the present study, air is treated as an ideal gas with isothermal properties, and the compressibility of water is governed by the following expressions for the density and density pressure derivative:

$$\rho = \rho_o + \frac{p}{c^2} \quad (1)$$

$$\frac{d\rho}{dp} = \frac{1}{c^2} \quad (2)$$

Here,  $\rho_o$  is a constant,  $p$  is the pressure, and  $c$  is the speed of sound. Lower values of sound speed can be used to improve the stability of the solution and accelerate convergence. However care must be taken to ensure that this artificial compressibility does not have a significant influence on the solution. Three different values for the speed of sound were tested, namely 100, 600 and 1450 m/s. The stability of the solution is assessed by monitoring the pressure scalar scenes and the time histories of pressure at different locations in the domain. The predicted pressure and deflection time histories for the panel with point supports are shown in Figure 6. Here zero time is when the keel edge touches the water surface.

Compressible flow models display a more stable solution, particularly for the lower values of sound speed. Some influence of artificial compressibility on the results can be observed for a sound speed of 100 m/s. In this case, the time scale of the impact event is of the same order as that of the sound transit time. An artificial sound speed of 600 m/s is concluded to be a good compromise between solution stability and accuracy for this particular test condition of 1 m/s impact velocity.

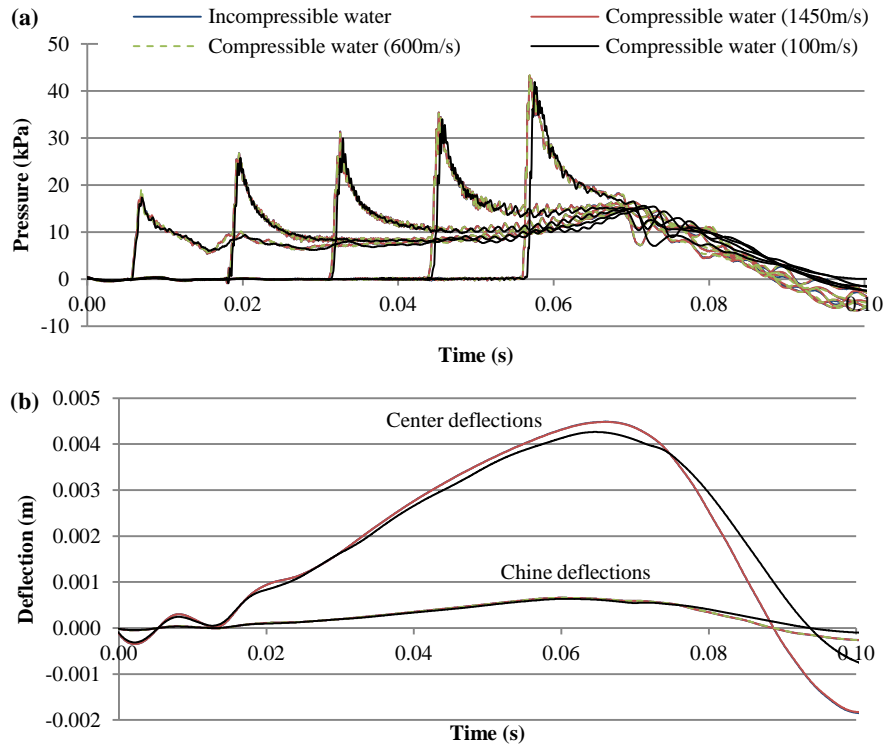


**Figure 6.** Influence of artificial compressibility on the (a) pressure and (b) center and chine deflection time histories.

#### 4.2. Influence of structural boundary conditions

The numerical and experimental pressure and deflection time histories are shown in Figure 7. The initial lowest peak is recorded by sensor P1, after which sensors P2 to P5 record progressively higher peaks due to the plate pushing water to the side, accelerating the fluid, as it penetrates the water at constant velocity. Maximum plate deflection occurs at the time the panel becomes fully immersed ( $t \approx 0.07$  s).

The numerical pressure time histories agree quite well, except for the slight difference in peak values at sensors P2 – P4. This can be explained by looking at the deflection time histories where significant differences are observed, both in terms of maximum deflection (up to 50%) and shape. As expected, a point support resulted in larger deflections at both the center and chine of the panel, leading to a larger reduction in the local impact velocity and associated fluid loading. Sensors P1 and P5 are located close to the boundaries where the deformation is small, resulting in only small changes in the local velocity. However, there is a slight discrepancy in peak pressure at sensor P5 (approximately 0.8 kPa). This is believed to be due to the small reduction in local deadrise angle at the chine as a result of the panel deformation.

The numerical model is well capable of predicting the pressure at different locations along the panel. Slight differences in the time of peak are attributed to the slight variations in the experimental impact velocity profile, whereas in the numerical model, the impact velocity is constant. However, the structural response is not well predicted. The point support model overpredicts the deflection at the center but gives reasonably good predictions near the chine, whereas the opposite is true for the area support model. In both cases, the numerical peak deflections occur a little later than in the experiments. It is clear that the experimental boundary conditions lie somewhere between these two cases tested, and a 3D model is required to accurately model the boundary conditions. In addition, the experimental results display an oscillatory behaviour after peak deflection, which, according to Allen [11] is due to the excitation of the panel at resonance. This is not captured by our numerical model, and is thought to be due to the numerical damping in the ABAQUS model.

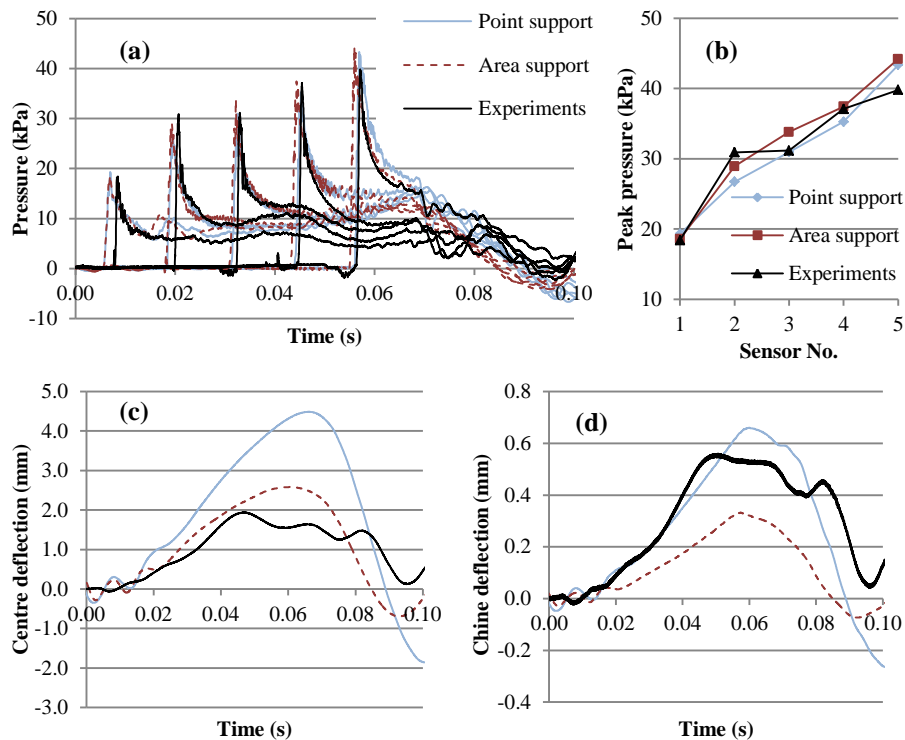


**Figure 7.** Effect of boundary conditions on the numerical (a, b) pressure and (c) center and (d) chine deflection time histories. Experimental results are also added for comparison.

### 4.3. Hydroelastic effects

Simulations with a rigid panel were also carried out to study the influence of hydroelastic effects on the fluid loading. The results are shown in Figure 8. The experimental results and the area support pressures are also included for comparison.

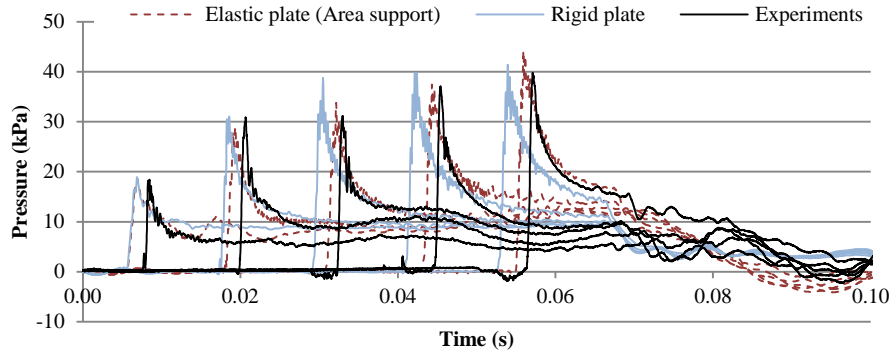


**Figure 8.** Influence of hydroelastic effects on the pressure time histories.

The influence of hydroelastic effects on the pressure time histories is not very clear. Some slight variations are observed at sensors P3 and P4, due to the change in local velocity as discussed earlier. The largest hydroelastic effect appears to be a time lag between the peak values, particularly at sensors P3 – P5. It is important to note that impact velocity considered in this paper is relatively low (1 m/s) for significant hydroelastic effects to be observed.

## 5. Conclusions

The constant velocity impact of a flexible panel with water is studied using two-way coupling of the commercial CFD software Star CCM+ and the FE software ABAQUS. A detailed description of the numerical model is given. It was concluded that due to the strong coupling between the fluid and structure, more iterations are needed to achieve convergence, with 20 iterations per time step being sufficient. The computational time can be improved by using convergence criteria for the pressure field instead of having a fixed number of iterations, which at certain times is overkill. The stability of the solution is further improved by treating the flow as compressible with a lower speed of sound to accelerate convergence, without affecting the solution.

Comparisons against published experimental data show that the model is well capable of predicting the fluid loading, for the test case investigated. However, the structural responses show less favorable agreement. The structural boundary conditions were found to have a significant influence on the deflection. Three-dimensional models are required to accurately model the experimental boundary conditions. Allen [11] showed that modelling the entire panel improves the prediction of panel deflections.

Preliminary investigations into the influence of hydroelastic effects were also carried out. The pressure time histories were compared with corresponding rigid body simulation results. No clear hydroelastic effects were observed, except for the slight delay in pressure rise time. Hydroelastic effects are small for these test conditions, in particular due to the low impact velocity considered. However, the aim at this stage was to set up a robust and reliable numerical model. Future work involves modelling

different test conditions, in terms of impact velocities and deadrise angles, and comparing the results, including deflection and strains, with corresponding rigid/quasi-static and one-way coupled simulations.

### Acknowledgments

The authors acknowledge the support of the Defence Science and Technology Laboratory (Dstl) in conducting the investigations for this paper. The authors would also like to thank Dr. Tom Allen for sharing his experimental data.

### References

- [1] O. Faltinsen, "Hydroelastic slamming," *Journal of Marine Science and Technology*, vol. 5, pp. 49–65, 2000.
- [2] A. Bereznitski, "Slamming: the role of hydroelasticity," *International Shipbuilding Progress*, vol. 4, no. 4, pp. 333–351, 2001.
- [3] I. Stenius, A. Rosén, and J. Kutteneuler, "Explicit FE-modelling of hydroelasticity in panel-water impacts," *International Shipbuilding Progress*, vol. 54, pp. 111–127, 2007.
- [4] K. J. Maki, D. Lee, A. W. Troesch, and N. Vlahopoulos, "Hydroelastic impact of a wedge-shaped body," *Ocean Engineering*, vol. 38, no. 4, pp. 621–629, Mar. 2011.
- [5] D. Piro and K. Maki, "Hydroelastic analysis of bodies that enter and exit water," *Journal of Fluids and Structures*, vol. 37, pp. 134–150, Feb. 2013.
- [6] I. Stenius, A. Rosén, and J. Kutteneuler, "Hydroelastic interaction in panel-water impacts of high-speed craft," *Ocean Engineering*, vol. 38, no. 2–3, pp. 371–381, Feb. 2011.
- [7] C. Lu, Y. He, and G. Wu, "Coupled analysis of nonlinear interaction between fluid and structure during impact," *Journal of fluids and structures*, vol. 14, pp. 127–146, 2000.
- [8] R. Panciroli, S. Abrate, G. Minak, and A. Zucchelli, "Hydroelasticity in water-entry problems: Comparison between experimental and SPH results," *Composite Structures*, vol. 94, no. 2, pp. 532–539, Jan. 2012.
- [9] K. Das and R. C. Batra, "Local water slamming impact on sandwich composite hulls," *Journal of Fluids and Structures*, vol. 27, no. 4, pp. 523–551, May 2011.
- [10] M. Battley, T. Allen, P. Pehrson, I. Stenius, and A. Rosén, "Effects of panel stiffness on slamming responses of composite hull panels," in *17th International Conference on Composite Materials, ICCM17*, 2009.
- [11] T. Allen, "Mechanics of flexible composite hull panels subjected to water impacts," University of Auckland, New Zealand, 2013.
- [12] H. Luo, H. Wang, and C. Guedes Soares, "Numerical and experimental study of hydrodynamic impact and elastic response of one free-drop wedge with stiffened panels," *Ocean Engineering*, vol. 40, pp. 1–14, Feb. 2012.
- [13] CD-adapco, *Star CCM+ User Guide Version 8.04*. 2013.
- [14] J. Camilleri, D. J. Taunton, and P. Temarel, "Slamming impact loads on high-speed craft sections using two-dimensional modelling," in *Analysis and Design of Marine Structures*, 2015, no. 2012, pp. 73–81.
- [15] D. Zenkert, *The handbook of sandwich construction*. EMAS, 1997.
- [16] D. Systèmes, *ABAQUS Documentation*, 6.13 ed. Providence, RI, USA, 2013.
- [17] C. Förster, W. A. Wall, and E. Ramm, "Artificial added mass instabilities in sequential staggered coupling of nonlinear structures and incompressible viscous flows," *Computer Methods in Applied Mechanics and Engineering*, vol. 196, no. 7, pp. 1278–1293, 2007.